Effective fecal microbiota transplantation for recurrent *Clostridioides difficile* infection in humans is associated with increased signalling in bile acid-farnesoid X receptor-fibroblast growth factor pathway

Tanya Monaghan*,[1] Benjamin H Mullish*,[2] Jordan Patterson,[3] Gane KS Wong,[3,4,8] Julian R Marchesi,[2,5] Huiping Xu,[6] Tahseen Jilani,[7] Dina Kao[8,9]

Short title: FMT acts on bile acid-FXR pathway

[1]NIHR Nottingham Biomedical Research Centre (BRC), Nottingham University Hospitals NHS Trust and the University of Nottingham, Nottingham, UK; [2]Division of Integrative Systems Medicine and Digestive Disease, Faculty of Medicine, Imperial College London, London, UK; [3]Department of Biological Sciences, University of Alberta, Edmonton, Alberta; [4]BGI-Shenzhen, Shenzhen, China; [5]School of Biosciences, Cardiff University, Cardiff, UK; [6]Department of Biostatistics, Indiana University; [7]School of Computer Science, Advanced Data Analysis Centre, University of Nottingham, Nottingham, UK; [8]Division of Gastroenterology, Department of Medicine, University of Alberta, Edmonton, Alberta; [9]Center of Excellence for Gastrointestinal Inflammation and Immunity Research, Edmonton, Alberta

*Joint first authors

Author contribution: TM, BHM, JRM and DK contributed to study design, data analysis and interpretation, drafting of manuscript and critical revision of manuscript. HX, JP, GKSW, and TJ contributed to data analysis, drafting of manuscript and critical revision of manuscript. TM and DK contributed equally to this manuscript.

Word count: 1906

Key words: microbiota; fecal microbiota transplantation (FMT); recurrent *Clostridium difficile* infection (rCDI); bile acid metabolism; fibroblast growth factor (FGF)19

Corresponding author:

Dina Kao, MD, FRCPC, Zeidler Ledcor Centre, Division of Gastroenterology, Department of Medicine, University of Alberta, Edmonton, Alberta

dkao@ualberta.ca

Abbreviations:

BMI	body mass index
CA	cholic acid
CDI	*Clostridioides difficile* infection
CDCA	chenodeoxycholic acid
DCA	deoxycholic acid
FGF	fibroblast growth factor
FMT	fecal microbiota transplantation
FXR	farnesoid X receptor
LCA	lithocholic acid
rCDI	recurrent *Clostridioides difficile* infection
NPX	Normalized Protein eXpression

ABSTRACT

The mechanisms of efficacy for fecal microbiota transplantation (FMT) in treating recurrent *Clostridioides difficile* infection (rCDI) remain poorly defined, with restored gut microbiota-bile acid interactions representing one possible explanation. Furthermore, the potential implications for host physiology of these FMT-related changes in gut bile acid metabolism are also not well explored. In this study, we investigated the impact of FMT for rCDI upon signalling through the farnesoid X receptor (FXR)-fibroblast growth factor (FGF) pathway. Herein, we identify that in addition to restoration of gut microbiota and bile acid profiles, FMT for rCDI is accompanied by a significant, sustained increase in circulating levels of FGF19 and reduction in FGF21. These FGF changes were associated with weight gain post-FMT, to a level not exceeding the pre-rCDI baseline. Collectively, these data support the hypothesis that the restoration of gut microbial communities by FMT for rCDI is associated with an upregulated FXR-FGF pathway, and highlight the potential systemic effect of FMT.

Introduction

Fecal microbiota transplantation (FMT) is a highly effective therapy against recurrent *Clostridioides difficile* infection (rCDI). However, the mechanisms by which FMT exerts its efficacy in rCDI remain unclear. In recent years, restoration of pre-morbid gut bile acid metabolism has become one of the better known potential mechanisms supported by both human and animal studies. Secondary bile acids inhibit *C. difficile* vegetative growth, while certain primary bile acids (and particularly taurocholic acid) promote germination.[1] It has been demonstrated that secondary bile acid concentrations are much reduced while primary bile acid levels are elevated in rCDI patients compared to healthy controls, potentially perpetuating *C. difficile* proliferation.[2] Following FMT, which restores the diversity and composition of the intestinal microbiota, bile

acid homeostasis is re-established.[2] Furthermore, there is also evidence that the loss of microbiota-derived bile-metabolising enzymes may contribute to the pathogenesis of CDI both in mice and in humans.[3–5]

Bile acid metabolism is not only regulated by commensal bacteria, but also through farnesoid X receptors (FXR), which are abundantly expressed in the liver and ileum.[6] In humans, the most potent endogenous ligand for FXR is the primary bile acid chenodeoxycholic acid (CDCA); the secondary bile acids deoxycholic acid (DCA) and lithocholic acid (LCA) are moderate FXR agonists, whilst the primary bile acid cholic acid (CA) also has modest agonist activity.[20] Upon ileal FXR activation, fibroblast growth factor (FGF)19 is secreted into the portal circulation, where it binds to the FGFR4/β Klotho receptor complex on hepatocytes. This interaction acts as both a negative feedback control on hepatic bile acid synthesis through inhibition, and also as a modulator of key metabolic pathways involved in glucose, lipid, and energy metabolism.[7] Although both FGF19 and FGF21 are involved in regulating multiple metabolic processes, they have an inverse relationship that collectively maintains metabolic homeostasis, since FGF19 is produced during feeding while FGF21 is secreted during fasting.[8] Perturbation of FXR signalling and altered FGF levels have been found in a number of disease states, including type 2 diabetes, metabolic syndrome and Crohn's disease.[9,10] Furthermore, surgically-induced weight loss is associated with an increase in FGF19 and a decrease in FGF21 levels.[9]

There is growing evidence from murine studies that altered interaction between the gut microbiota and bile acids may directly affect FXR signalling. Germ-free and antibiotic-treated mice have markedly reduced ileal *Fgf15* gene expression (murine orthologue of human FGF19).[11]

The resultant accumulation of tauro-β-muricholic acid (an FXR antagonist) is thought to be the link between alterations of the gut microbiota and FXR signalling in mice. However, given that this bile acid is only present at very modest levels in humans, coupled with the differences in FGF orthologues and microbiota between humans and mice, extrapolating these data to humans is problematic. Presently, there are no human studies to our knowledge examining the impact of antibiotic-induced dysbiosis on FXR signalling. Given the apparent key contribution of the microbiota-bile acid axis to CDI pathogenesis, we investigated the association between changes in bile acid composition and FGF19 and 21 following FMT for the treatment of rCDI in humans. To do this, we analysed samples collected from a recent randomised trial of capsulized vs colonoscopic FMT for the treatment of rCDI.[12] We undertook metagenomic, metabonomic and proteomic analyses for these samples, and correlated with weight changes following rCDI eradication.

Results

a) Stool metagenome analysis

We have previously described that successful FMT for rCDI is associated with both marked increases in stool microbial diversity and altered microbial community composition to resemble that of healthy donors, maintained up to at least 12 weeks post-FMT.[12] Further analysis here demonstrated that successful FMT was particularly associated with enrichment of a number of bacterial genera including *Bacteroides, Faecalibacterium, Ruminococcus, Blautia* and *Eubacterium* (all of which contain members with bile acid-metabolising function) and loss of *Klebsiella, Escherichia* and *Veillonella* (which generally lack these functions) (**Supplementary Figure 1**).[20]

b) Ultra-performance liquid chromatography-mass spectrometry (UPLC-MS) stool bile acid profiling

Successful FMT was also associated with significantly decreased stool levels of the primary bile acids CDCA and CA, and significantly increased levels of the secondary bile acids DCA and LCA (**Figure 1**). In all cases, these changes were observed at four weeks post-FMT and were maintained at 12 weeks post-therapy.

c) Proteomic analysis

Of 73 compared proteomic markers (**Supplementary Table 1**), the differences were statistically significant for only two: FGF19 and FGF21 (**Figure 2**). FGF19 had significantly higher Normalized Protein eXpression (NPX) values at weeks 4 and 12 compared with screening, while FGF21 had significantly lower NPX values at weeks 4 and 12 compared with screening. There was no significant difference in the levels of FGF19 and FGF21 between the groups receiving FMT by either capsules or colonoscopy (data not shown).

d) Differences in weight before and after FMT

Following successful FMT, there was a statistically significant increase in mean BMI at 12 weeks following FMT compared to screening, but this did not exceed pre-rCDI baseline (mean BMI difference [95%CI], 0.5 [0.2, 0.8]; p = 0.003, **Table 1**.

Discussion

While it has already been observed that FMT in humans with rCDI restores gut microbiota and bile acid composition, we demonstrate for the first time that this procedure is also associated with activation of ileal FXR signalling, manifested by increased FGF19 and reduced FGF21 expression. CDCA is the most potent endogenous ligand for FXR, although the secondary bile acids DCA and LCA are also moderate FXR agonists. Our data suggest that the reduced level of a potent FXR agonist (CDCA) is offset by increased levels of two moderate FXR agonists (DCA and LCA),[21] with a net upregulation of the ileal FXR-FGF pathway following successful FMT. Some phases of this bile acid transformation process (e.g. 7-α dehydroxylation) occur within the colon, implying that for secondary bile acids to affect ileal FXR signaling, they must be reabsorbed in the colon and re-secreted in bile into the small intestine.[22] Although metabolism of bile acids in the gut is a bacterially-driven process,[20] further studies are needed to examine the specific contribution of different bacteria to this process.

In addition to its well-defined roles in the regulation of metabolism and bile acid production, there is also evidence in how FXR signalling plays a role in other systemic processes relevant to CDI. For example, FXR activation has been shown to inhibit bacterial overgrowth and block mucosal injury in mouse ileum,[23] and is associated with reduced expression of key cytokines (including TNF-α and IL-1β) that regulate the host innate immune response.[24] Moreover, the inflammatory response or *C. difficile* itself could reciprocally inhibit activation of FXR and its target FGF genes, and this therefore merits further study.

Although our data are consistent with previous studies in observing restoration of the gut microbiota and bile acid composition post-FMT for rCDI, there is no direct demonstration that this

pathway is a key mechanism underpinning the efficacy of FMT for rCDI. In addition, it is not clear if the observed weight gain following FMT is directly mediated through changes in FGF19/21 levels. Future mechanistic studies involving mouse models of CDI would be required to determine causality, and such studies should consider including analysis of the effect of FMT upon FXR signalling. Should these experiments validate our preliminary findings, the bile acid-FXR axis may become a novel therapeutic target for the treatment of rCDI. There are already some data that would appear to support this strategy; specifically, the potent FXR agonist obeticholic acid (INT-747) has been shown to display anti-*C. difficile* potential in murine models of CDI.[25] However, the benefits and risks of synthetic FXR ligands require further evaluation.

In conclusion, our data suggest that FMT is associated with upregulation of the bile acid-FXR-FGF signalling pathway, and this may possibly explain the rapid improvement in energy and well-being many patients experience following FMT. Although these findings are intriguing, we acknowledge several limitations, including small sample size, short follow-up period, the observational nature of the data, lack of mucosal inflammatory protein expression data, and non-consideration of diet or host genetics. Insights gleaned from better understanding of FMT mechanisms of action using a multi-omics approach could enable development of tailored therapies that target key signaling pathways or specific constituents of those pathways that may regulate host defence to circumvent various concerns surrounding FMT.

Materials and Methods

a) Patient clinical data, sample collection and storage

Participants (*n*=116) in the capsule vs colonoscopy-delivered FMT trial were included this pilot study.[12] Blood and stool samples were collected, and body mass indices (BMI) documented at screening and subsequent follow-up visits at weeks 4 and 12 after FMT. Of the 64 patients recruited from Edmonton, 43 had complete sets of archived blood samples and were subjected to proteomic analyses using the Olink inflammation panel. Of these 43 patients, 23 were chosen at random to have their stool samples undergo microbial composition analysis by shotgun metagenomics sequencing. From these 23 patients, 17 randomly-selected patients had stool bile acid profiling by ultra-performance liquid chromatography-mass spectrometry (UPLC-MS). Patient baseline characteristics are shown in **Table 2**. The metagenomic, metabonomic, and proteomic results were correlated with weight changes following rCDI eradication. This study was approved by the research ethics board of the University of Alberta (Pro49006).

b) Stool metagenomics

Whole-genome shotgun sequencing was performed as previously described.[12] More specifically, taxonomic classification of reads from each library was conducted with Kraken.[13] The database used consisted of all bacteria, archaea, viruses, fungi, and protozoa full-length genomes from NCBI RefSeq, the human genome assembly GRCh38, and reference bacterial assemblies from the Human Microbiome Project.[14] Read assignments were filtered with Kraken-filter using a threshold of 10%.

c) UPLC-MS profiling of fecal bile acids

Sample preparation was performed using protocols as previously-described.[15] Bile acid analysis of faecal extracts was performed using ACQUITY UPLC (Waters Ltd, Elstree, UK) coupled to a

Xevo G2 Q-ToF mass spectrometer equipped with an electrospray ionization source operating in negative ion mode (ESI-), using the method described by Sarafian and colleagues.[16] Waters raw data files were converted to NetCDF format and data extracted using the XCMS (v1.50) package in R (v3.1.1) software. Probabilistic quotient normalisation[17] was used to correct for dilution effects and chromatographic features with coefficient of variation higher than 30% in the QC samples were excluded from further analysis. The relative intensities of the features were corrected to the dry weight of the faecal samples.

d) Proteomics

The relative levels of serum inflammatory proteins were analyzed with Olink® Inflammation I panel (Olink Proteomics AB, Uppsala, Sweden) using Proximity Extension Assay (PEA) according to the manufacturer's instructions.[18,19] A list of the 92 inflammation-related markers is listed in **Supplementary Table 2**. In brief, serum samples (1µL) were incubated with 92 oligonucleotide labelled antibody probe pairs that bind to their respective target in the sample. A PCR reporter sequence was formed by a proximity dependent DNA polymerization event and was subsequently detected and amplified using a microfluidic real-time PCR instrument (Biomark HD, Fluidigm). Data was then quality controlled and normalized using an internal extension control and an inter-plate control, to adjust for intra- and inter-run variation. The final assay read-out is presented in Normalized Protein eXpression (NPX) values, which is an arbitrary unit on a log2-scale where a high value corresponds to a higher protein expression. All assay validation data (detection limits, intra- and inter-assay precision data, etc) are available on the manufacturer's website (http://www.olink.com). Samples failing technical quality controls or that fell below lower limits of detection were excluded from analyses.

e) Statistical Analysis

Full methodology for statistical analysis is provided in the **Supplementary Material.**

Funding

This work was supported by University of Nottingham under Grant RPA22082017; Alberta Health Services under Grant 0022725; University of Alberta Hospital Foundation under Grant 3630; Medical Research Council Clinical Research Training Fellowship under Grant MR/R000875/1; Division of Integrative Systems Medicine and Digestive Disease at Imperial College London receive financial support from the National Institute of Health Research (NIHR) Imperial Biomedical Research Centre (BRC) based at Imperial College Healthcare NHS Trust and Imperial College London.

References

1. Thanissery R, Winston JA, Theriot CM. Inhibition of spore germination, growth, and toxin activity of clinically relevant C. difficile strains by gut microbiota derived secondary bile acids. *Anaerobe*. 2017;45:86-100. doi:10.1016/j.anaerobe.2017.03.004.

2. Weingarden AR, Chen C, Bobr A, et al. Microbiota transplantation restores normal fecal bile acid composition in recurrent Clostridium difficile infection. *AJP Gastrointest Liver Physiol*. 2014;306(4):G310-G319. doi:10.1152/ajpgi.00282.2013.

3. Allegretti JR, Kearney S, Li N, et al. Recurrent Clostridium difficile infection associates with distinct bile acid and microbiome profiles. *Aliment Pharmacol Ther*. 2016;43(11):1142-1153. doi:10.1111/apt.13616.

4. Buffie CG, Bucci V, Stein RR, et al. Precision microbiome reconstitution restores bile acid mediated resistance to Clostridium difficile. *Nature*. 2014;517(7533):205-208.

doi:10.1038/nature13828.

5. Studer N, Desharnais L, Beutler M, et al. Functional Intestinal Bile Acid 7α-Dehydroxylation by Clostridium scindens Associated with Protection from Clostridium difficile Infection in a Gnotobiotic Mouse Model. *Front Cell Infect Microbiol*. 2016;6:191. doi:10.3389/fcimb.2016.00191.

6. Lefebvre P, Cariou B, Lien F, Kuipers F, Staels B. Role of Bile Acids and Bile Acid Receptors in Metabolic Regulation. *Physiol Rev*. 2009;89(1):147-191. doi:10.1152/physrev.00010.2008.

7. Benoit B, Meugnier E, Castelli M, et al. Fibroblast growth factor 19 regulates skeletal muscle mass and ameliorates muscle wasting in mice. *Nat Med*. 2017;23(8):990-996. doi:10.1038/nm.4363.

8. Zhang F, Yu L, Lin X, et al. Minireview: Roles of Fibroblast Growth Factors 19 and 21 in Metabolic Regulation and Chronic Diseases. *Mol Endocrinol*. 2015;29(10):1400-1413. doi:10.1210/me.2015-1155.

9. Gómez-Ambrosi J, Gallego-Escuredo JM, Catalán V, et al. FGF19 and FGF21 serum concentrations in human obesity and type 2 diabetes behave differently after diet- or surgically-induced weight loss. *Clin Nutr*. 2017;36(3):861-868. doi:10.1016/j.clnu.2016.04.027.

10. Nolan JD, Johnston IM, Pattni SS, Dew T, Orchard TR, Walters JR. Diarrhea in Crohn's Disease: Investigating the Role of the Ileal Hormone Fibroblast Growth Factor 19. *J Crohn's Colitis*. 2015;9(2):125-131. doi:10.1093/ecco-jcc/jju022.

11. Sayin SI, Wahlström A, Felin J, et al. Gut Microbiota Regulates Bile Acid Metabolism by Reducing the Levels of Tauro-beta-muricholic Acid, a Naturally Occurring FXR Antagonist. *Cell Metab*. 2013;17(2):225-235. doi:10.1016/j.cmet.2013.01.003.

12. Kao D, Roach B, Silva M, et al. Effect of Oral Capsule– vs Colonoscopy-Delivered Fecal Microbiota Transplantation on Recurrent *Clostridium difficile* Infection. *JAMA*. 2017;318(20):1985. doi:10.1001/jama.2017.17077.

13. Wood DE, Salzberg SL. Kraken: ultrafast metagenomic sequence classification using exact alignments. *Genome Biol*. 2014;15(3):R46. doi:10.1186/gb-2014-15-3-r46.

14. Gevers D, Knight R, Petrosino JF, et al. The Human Microbiome Project: A Community Resource for the Healthy Human Microbiome. *PLoS Biol*. 2012;10(8):e1001377. doi:10.1371/journal.pbio.1001377.

15. Mullish BH, Pechlivanis A, Barker GF, Thursz MR, Marchesi JR, McDonald JAK. Functional microbiomics: Evaluation of gut microbiota-bile acid metabolism interactions in health and disease. *Methods*. 2018. doi:10.1016/j.ymeth.2018.04.028.

16. Sarafian MH, Lewis MR, Pechlivanis A, et al. Bile Acid Profiling and Quantification in Biofluids Using Ultra-Performance Liquid Chromatography Tandem Mass Spectrometry. *Anal Chem*. 2015;87(19):9662-9670. doi:10.1021/acs.analchem.5b01556.

17. Veselkov KA, Vingara LK, Masson P, et al. Optimized Preprocessing of Ultra-Performance Liquid Chromatography/Mass Spectrometry Urinary Metabolic Profiles for Improved Information Recovery. *Anal Chem*. 2011;83(15):5864-5872. doi:10.1021/ac201065j.

18. Assarsson E, Lundberg M, Holmquist G, et al. Homogenous 96-Plex PEA Immunoassay

Exhibiting High Sensitivity, Specificity, and Excellent Scalability. Hoheisel JD, ed. *PLoS One*. 2014;9(4):e95192. doi:10.1371/journal.pone.0095192.

19. Lundberg M, Eriksson A, Tran B, Assarsson E, Fredriksson S. Homogeneous antibody-based proximity extension assays provide sensitive and specific detection of low-abundant proteins in human blood. *Nucleic Acids Res*. 2011;39(15):e102-e102. doi:10.1093/nar/gkr424.

20. Wahlström A, Sayin SI, Marschall H-U, Bä Ckhed F. Intestinal Crosstalk between Bile Acids and Microbiota and Its Impact on Host Metabolism. *Cell Metab*. 2016;24:41-50. doi:10.1016/j.cmet.2016.05.005.

21. Parks DJ, Blanchard SG, Bledsoe RK, et al. Bile acids: natural ligands for an orphan nuclear receptor. *Science*. 1999;284(5418):1365-1368. doi:10.1126/SCIENCE.284.5418.1365.

22. Ridlon JM, Kang D-J, Hylemon PB. Bile salt biotransformations by human intestinal bacteria. *J Lipid Res*. 2006;47(2):241-259. doi:10.1194/jlr.R500013-JLR200.

23. Inagaki T, Moschetta A, Lee Y-K, et al. Regulation of antibacterial defense in the small intestine by the nuclear bile acid receptor. *Proc Natl Acad Sci*. 2006;103(10):3920-3925. doi:10.1073/pnas.0509592103.

24. Vavassori P, Mencarelli A, Renga B, Distrutti E, Fiorucci S. The Bile Acid Receptor FXR Is a Modulator of Intestinal Innate Immunity. *J Immunol*. 2009;183(10):6251-6261. doi:10.4049/jimmunol.0803978.

25. Tessier MEM, Andersson H, Ross C, et al. Mo1850 Obeticholic Acid (INT-747) Confers Disease Protection Against Clostridium difficile Infection. *Gastroenterology*.

2015;148(4):S-726. doi:10.1016/S0016-5085(15)32479-3.

Figure 1. **Effect of FMT for rCDI upon bile acid profiles.** A significant decrease in chenodeoxycholic acid (A) and cholic acid (B) is seen between screening and 4 weeks, and maintained up to 12 weeks post-FMT. A significant increase in lithocholic acid (C) and deoxycholic acid (D) is observed between screening and 4 weeks, and maintained up to 12 weeks post-FMT. X-axis depicts time, and y-axis depicts relative intensity of each bile acid. Pre-FMT = screening; week 4 = 4 weeks after fecal microbiota transplantation (FMT); week 12 = 12 weeks post-FMT.

Figure 2. Normalized Protein eXpression (NPX) values for serum fibroblast growth factor (FGF)19 (A) and FGF21 (B) over time. There is a statistically significant increase in FGF19 level 4 and 12 weeks after FMT compared to screening, while a statistically significant decrease in FGF21 level is observed 4 and 12 weeks following FMT. X-axis depicts time, and y-axis depicts relative quantification of respective FGF. Circles represent mean; error bars represent standard deviation.

Table 1. Comparison of the mean body mass index (BMI) over time. At week 4, the mean BMI was not significantly different from the mean BMI prior to FMT. At week 12, patients had significantly higher BMI relative to pre-FMT, but did not exceed pre-rCDI baseline.

	Mean BMI Difference (95% CI)	***p* value**
Week 4 - Pre-FMT	0.0 (-0.3, 0.3)	0.84
Week 12 - Pre-FMT	0.5 (0.2, 0.8)	0.003
Week 12 - Week 4	0.4 (0.1, 0.8)	0.006

Table 2. Patient baseline characteristics

Variable	Blood proteomics analysis (n=43)	Stool bile acid analysis (n=17)
Age, mean (SD), y	58.8 (19.2)	58.1 (17.1)
Female, No. (%)	27 (62.8%)	13 (76%)
Charlson Comorbidity Index score, median (Q1-Q3)	3 (1-5)	3 (1-4)
Immunosuppressed patients, No. (%)	5 (11.6%)	0
BMI, mean (SD)	25.9 (5.9)	27.5 (6.0)
PPI use prior to FMT, No. (%)	5 (11.6%)	2 (11.7%)
Hemoglobin, median (Q1-Q3), g/dL	13.8 (13.0-14.4)	13.9 (13.1-14.5)
White blood cell count, median (Q1-Q3), /uL	7100 (5850-8500)	6750 (5620-8130)
Albumin, median (Q1-Q3), g/dL	4.0 (3.8-4.3)	4.0 (3.9-4.3)
C-reactive protein, median (Q1-Q3), mg/dL	0.29 (0.085-0.10)	0.30 (0.075-0.89)
Creatinine, median (Q1-Q3), mg/dL	0.75 (0.66-0.87)	0.74 (0.66-0.94)
Capsule delivered FMT, No. (%)	25 (58.1%)	11 (64.7%)

Abbreviations: BMI, body mass index; FMT, fecal microbiota transplantation; PPI, proton pump inhibitor; Q1, first quartile; Q3, third quartile.

Figure

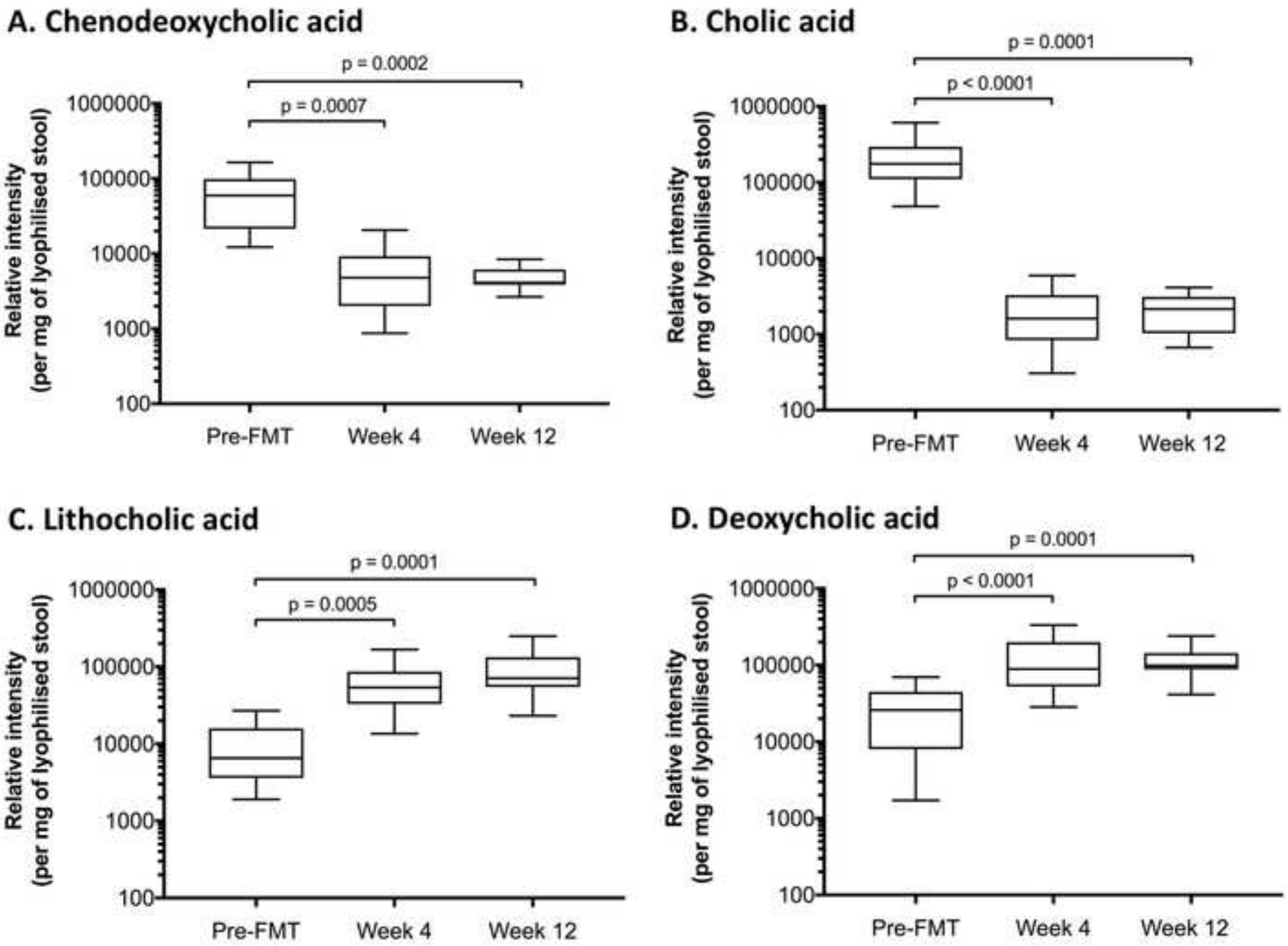
A. Chenodeoxycholic acid
p = 0.0002
p = 0.0007
Relative intensity (per mg of lyophilised stool)
1000000
100000
10000
1000
100
Pre-FMT
Week 4
Week 12
B. Cholic acid
p = 0.0001
p < 0.0001
Relative intensity (per mg of lyophilised stool)
1000000
100000
10000
1000
100
Pre-FMT
Week 4
Week 12
C. Lithocholic acid
p = 0.0001
p = 0.0005
Relative intensity (per mg of lyophilised stool)
1000000
100000
10000
1000
100
Pre-FMT
Week 4
Week 12
D. Deoxycholic acid
p = 0.0001
p < 0.0001
Relative intensity (per mg of lyophilised stool)
1000000
100000
10000
1000
100
Pre-FMT
Week 4
Week 12

Figure

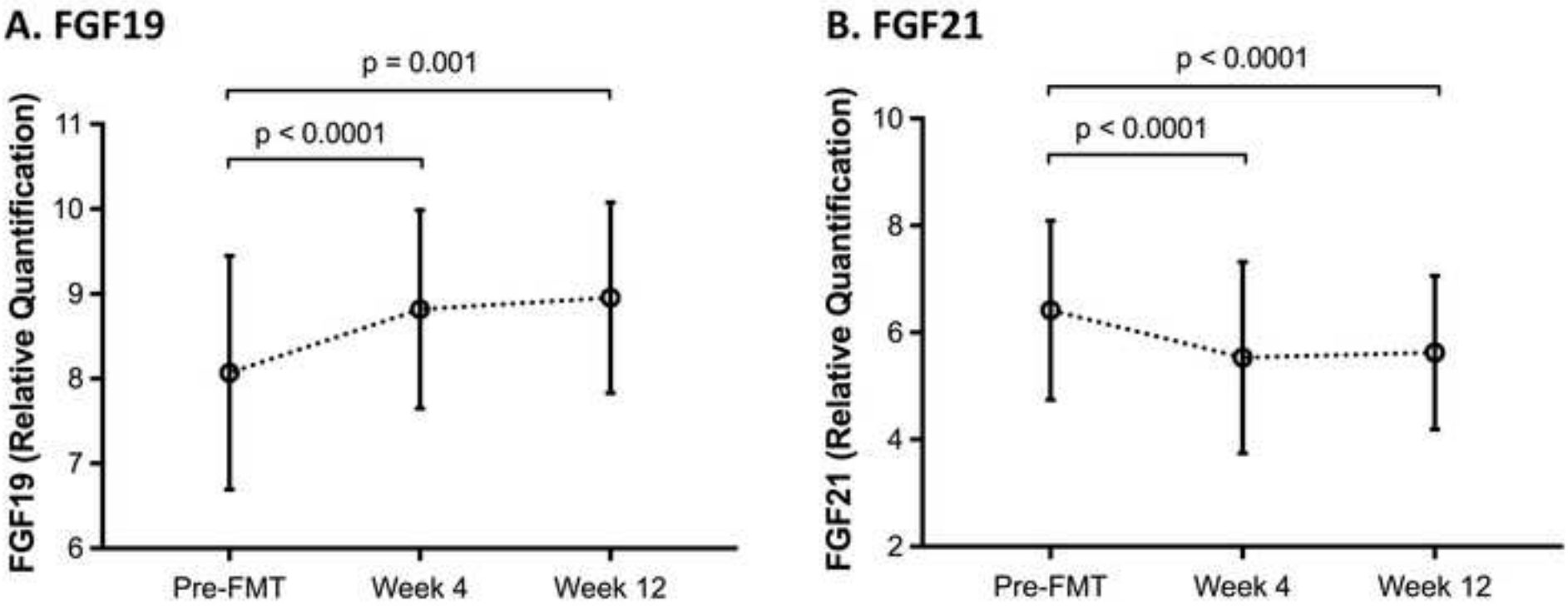
A. FGF19
p = 0.001
p < 0.0001
FGF19 (Relative Quantification)
11
10
9
8
7
6
Pre-FMT
Week 4
Week 12
B. FGF21
p < 0.0001
p < 0.0001
FGF21 (Relative Quantification)
10
8
6
4
2
Pre-FMT
Week 4
Week 12

Supplementary Figure 1:

Effective fecal microbiota transplantation for recurrent *Clostridium difficile* infection in humans is associated with increased signalling in bile acid-farnesoid X receptor-fibroblast growth factor pathway

Supplementary material:

1. Materials and methods

1.1.Sample collection and storage

Whole blood samples were collected and initially stored at room temperature for up to 2 hours before being centrifuged for ten minutes at 1.5 RCF (relative centrifugal force). The serum samples were subsequently transferred to new collection tubes and stored at -80º C before proteomics profiling. Stool samples were collected by patients at home and stored at 4^0C for up to 8 hours; these samples were aliquoted and stored at -80º C before further analyses.

1.2.Statistical Analysis

Changes in BMI over time were analyzed using the mixed effects model with SAS version 9.4 (SAS Institute).

For metagenomic data analysis, genus-level extended error bar plots were generated using the Statistical Analysis of Metagenomic Profiles (STAMP) software package using White's non-parametric *t*-test with Benjamini-Hochberg FDR correction.[1]

Of the 92 proteins measured (**Supplementary Table 2**), 19 appeared to be below the detection limit for > 25% of the samples and thus were excluded from the analysis. For each group undergoing proteomic analysis, mean values with standard deviation and 95% group confidence intervals of protein expression of 73/92 investigated inflammation-associated markers were determined. Systematic changes in protein levels between time points (screening *vs* 4 weeks *vs* 12 weeks post FMT) were examined using a general linear model repeated-

measures ANOVA. The threshold for statistical significance was set at an alpha = 0.01. Wilk's Lambda test for multivariate comparison of time points [indicates whether or not the within-subject means of more than two groups (time points) are statistically significant and where the null hypothesis is rejected if the Wilk's lamda is small or close to zero] and Greenhouse-Geisser Epilson tests for Sphericity were performed. The Bonferroni method was used to adjust for multiple comparisons between time points and adjusted *p* values have been presented in **Supplementary Table 1.** For residual analysis, Shapiro-Wilk's test for residual normality and visual inspection of residual plots plotted against fitted values for heteroscedasticity were also performed. Statistical analyses were conducted using IBM SPSS statistic package version 22 (IBM, Armonk, New York, USA).

For bile acid data, pre-FMT and post-FMT samples were compared Wilcoxon Rank-Sum test where *p* values less than 0.05 were considered as statistically significant. Statistical analyses were carried out using GraphPad Prism 7 software (GraphPad Software, USA).

Supplementary Figure 1: Effect of FMT for rCDI upon genus-level gut microbial profiles. Extended error bar plots, with genera changing significantly measured by White's non-parametric test with Benjamini-Hochberg correction, using threshold between mean proportions of >1%. (A) pre-FMT vs 4 weeks post-FMT; (B) pre-FMT vs 12 weeks post-FMT.

Supplementary Table 1: Effect of FMT for rCDI upon Normalised Protein Expression Units (NPX) values with Bonferroni correction (alpha = 0.01). Pre-FMT vs 4 weeks post-FMT; Pre-FMT vs 12 weeks post FMT; week 4 vs week 12 post-FMT by repeated-measures ANOVA.

Supplementary Table 2. **List of 92 proteins measured by high-throughput, multiplex immunoassays Inflammation I panel by Olink®** (Olink Proteomics AB, Uppsala, Sweden)

Supplementary References:

1. Parks DH, Tyson GW, Hugenholtz P, Beiko RG. STAMP: statistical analysis of taxonomic and functional profiles. Bioinformatics (Oxford, England) 2014; 30:3123-4.

Supplementary Table 1. Effect of FMT for rCDI upon Normalised Protein Expression Units (NPX) values with Bonferroni correction (alpha = 0.01). Pre-FMT vs 4 weeks post-FMT; Pre-FMT vs 12 weeks post FMT; week 4 vs week 12 post-FMT by repeated-measures ANOVA.

Protein	Time Point			Repeated Measure ANOVA	Multiple Comparision p-values (Bonferroni Correction, α=0.01)		
	Pre-FMT	Week4	week12	Wilk's Lambda test (p-values)	Pre FMT - Week4	Pre FMT - Week12	Week4 - Week12
IL8	10.90(1.94)	10.58(1.63)	10.42(2.16)	0.729	0.753	0.940	1.000
VEGFA	10.65(0.64)	10.58(0.65)	10.65(0.69)	0.847	1.000	1.000	1.000
MCP-3	4.87(1.7)	4.53(1.5)	4.29(1.76)	0.311	0.438	0.594	1.000
GDNF	1.02(0.56)	0.9(0.5)	0.91(0.51)	0.311	0.465	0.574	0.465
CDCP1	3.6(1.03)	3.56(0.99)	3.54(1.03)	0.962	1.000	1.000	1.000
CD244	6.38(0.32)	6.33(0.36)	6.31(0.38)	0.728	1.000	1.000	1.000
IL7	3.92(0.95)	3.81(0.97)	3.93(0.99)	0.940	1.000	1.000	1.000
OPG	10.85(0.51)	10.73(0.54)	10.8(0.56)	0.657	1.000	1.000	1.000
LAP TGF-beta-1	8.33(0.3)	8.3(0.33)	8.29(0.31)	0.736	1.000	1.000	1.000
uPA	10.41(0.41)	10.4(0.46)	10.4(0.45)	0.899	1.000	1.000	1.000
IL6	4.39(1.77)	4.02(1.19)	4.18(1.83)	0.475	0.655	1.000	1.000
IL-17C	1.19(0.79)	1.11(1.03)	1.12(0.86)	0.622	1.000	0.984	1.000
MCP-1	10.8(0.62)	10.75(0.73)	10.65(0.52)	0.607	1.000	0.988	1.000
CXCL11	8.97(0.69)	8.99(0.93)	8.71(0.81)	0.026	1.000	0.045	0.311
AXIN1	4.88(0.47)	4.86(0.46)	4.82(0.7)	0.859	1.000	1.000	1.000
TRAIL	8.23(0.39)	8.23(0.35)	8.23(0.31)	0.847	1.000	1.000	1.000
CXCL9	8.03(1.24)	7.92(1.53)	7.77(1.32)	0.625	1.000	1.000	1.000
CST5	6.3(0.87)	6.35(0.78)	6.44(1.01)	0.512	1.000	0.730	1.000
OSM	5.86(0.97)	5.98(0.91)	6.09(1.04)	0.475	1.000	0.685	1.000
CXCL1	8.25(0.91)	8.03(0.63)	8(0.86)	0.232	0.346	0.287	1.000
CCL4	7.85(0.75)	7.77(0.74)	7.76(0.83)	0.56	1.000	0.837	1.000
CD6	5.05(0.6)	5.14(0.72)	5.25(0.58)	0.25	0.988	0.316	1.000
SCF	9.87(0.43)	9.75(0.44)	9.82(0.34)	0.341	0.532	0.072	0.055
IL18	8.24(0.62)	8.21(0.53)	8.07(0.56)	0.031	1.000	0.096	0.037
SLAMF1	1.94(0.67)	1.96(0.57)	1.9(0.66)	0.905	1.000	1.000	1.000
TGF-alpha	3.49(0.62)	3.69(0.56)	3.73(0.58)	0.121	0.143	0.189	1.000
MCP-4	4.69(0.53)	4.53(0.56)	4.58(0.58)	0.457	0.696	1.000	1.000
CCL11	8.29(0.53)	8.31(0.51)	8.43(0.49)	0.414	1.000	0.545	1.000
TNFSF14	7.17(0.63)	7.21(0.6)	7.18(0.75)	0.825	1.000	1.000	1.000

FGF-23	1.86(1.67)	1.73(1.56)	1.85(1.65)	0.437	1.000	1.000	0.833
IL-10RA	1.46(0.88)	1.44(0.87)	1.25(0.37)	0.881	1.000	1.000	1.000
FGF-5	1.31(0.32)	1.31(0.35)	1.31(0.39)	0.644	1.000	1.000	1.000
MMP-1	14.3(0.78)	14.34(0.76)	14.22(0.9)	0.66	1.000	1.000	1.000
LIF-R	3.06(0.35)	3.03(0.39)	3.04(0.38)	0.908	1.000	1.000	1.000
FGF-21	6.42(1.67)	5.53(1.79)	5.63(1.43)	<0.0001	<0.0001	<0.0001	1.000
CCL19	9(1.11)	8.97(1.09)	8.82(1.17)	0.621	1.000	1.000	1.000
IL-15RA	0.51(0.36)	0.45(0.36)	0.46(0.33)	0.690	1.000	1.000	1.000
IL-10RB	7(0.45)	6.93(0.43)	6.99(0.48)	0.949	1.000	1.000	1.000
IL-18R1	7.11(0.54)	7.14(0.6)	7.15(0.57)	0.974	1.000	1.000	1.000
PD-L1	4.11(0.66)	4.04(0.65)	3.94(0.71)	0.241	1.000	0.363	0.488
Beta-NGF	1.78(0.31)	1.7(0.34)	1.64(0.37)	0.114	0.521	0.109	0.657
CXCL5	11.22(1.36)	11.15(1.15)	10.92(1.19)	0.326	1.000	0.475	0.737
TRANCE	4.25(0.66)	4.11(0.61)	3.93(0.55)	0.025	0.605	0.019	0.583
HGF	8.94(0.56)	8.89(0.51)	8.99(0.55)	0.777	1.000	1.000	1.000
IL-12B	4.72(0.73)	4.47(0.92)	4.47(0.93)	0.025	0.071	0.063	1.000
MMP-10	6.2(0.82)	6.12(0.91)	6.1(0.74)	0.471	1.000	0.901	0.920
IL10	3.18(0.85)	3.24(0.85)	3.17(0.84)	0.634	1.000	1.000	1.000
CCL23	10.03(0.53)	9.81(0.67)	9.8(0.64)	0.106	0.226	0.181	0.226
CD5	5.4(0.49)	5.37(0.62)	5.48(0.5)	0.58	1.000	0.900	1.000
CCL3	5.93(1.13)	5.76(0.88)	5.8(1.25)	0.604	1.000	1.000	1.000
Flt3L	9.02(0.6)	9.07(0.57)	9(0.63)	0.226	0.324	1.000	0.925
CXCL6	8.28(0.86)	8.19(0.62)	7.9(0.83)	0.03	0.845	0.038	0.047
CXCL10	8.49(0.77)	8.5(1.13)	8.26(1.06)	0.239	1.000	0.422	0.468
4E-BP1	9.23(1.05)	9.21(1.25)	9.46(1.23)	0.382	1.000	0.488	1.000
SIRT2	4.84(0.55)	4.82(0.94)	4.91(0.92)	0.774	1.000	1.000	1.000
CCL28	2.05(0.62)	1.94(0.53)	1.94(0.57)	0.648	1.000	1.000	1.000
DNER	8.16(0.35)	8.17(0.29)	8.13(0.32)	0.582	0.902	1.000	1.000
EN-RAGE	5.42(1.15)	5.52(1.02)	5.35(1.02)	0.571	0.958	1.000	1.000
CD40	11.28(0.43)	11.18(0.49)	11.24(0.48)	0.505	0.818	1.000	1.000
FGF-19	8.07(1.38)	8.82(1.17)	8.95(1.12)	<0.0001	<0.0001	0.001	1.000
MCP-2	8.42(0.63)	8.48(0.81)	8.37(0.72)	0.648	1.000	1.000	1.000
CASP-8	4.4(0.62)	4.24(0.57)	4.32(0.57)	0.512	0.748	1.000	1.000
CCL25	6.28(0.72)	6.3(0.85)	6.46(0.72)	0.294	1.000	0.384	1.000
CX3CL1	5.8(0.61)	5.69(0.64)	5.64(0.73)	0.731	1.000	1.000	1.000
TNFRSF9	6.88(0.9)	6.56(0.93)	6.7(0.99)	0.049	0.042	0.387	0.042
NT-3	1.14(0.57)	1.14(0.64)	1.07(0.75)	0.947	1.000	1.000	1.000
TWEAK	9.95(0.43)	9.88(0.4)	9.83(0.4)	0.738	1.000	1.000	1.000
STAMPB	5.42(0.52)	5.41(0.79)	5.51(0.8)	0.576	1.000	0.880	1.000
CCL20	4.42(1.19)	4.47(1.41)	4.41(0.94)	0.69	1.000	1.000	1.000
ST1A1	6.11(0.6)	6.03(0.56)	5.85(0.63)	0.063	1.000	0.092	0.338

ADA	4.42(0.52)	4.39(0.61)	4.29(0.46)	0.516	1.000	0.742	1.000
TNFB	3.94(0.49)	3.93(0.53)	3.9(0.6)	0.73	1.000	1.000	1.000
CSF-1	8.29(0.29)	8.27(0.31)	8.27(0.32)	0.757	1.000	1.000	1.000

Supplementary Table 2. List of 92 proteins measured by high-throughput, multiplex immunoassays Inflammation I panel by Olink® (Olink Proteomics AB, Uppsala, Sweden)

Target	Abbreviated form
Adenosine Deaminase	ADA
Artemin	ARTN
Axin-1	AXIN1
Beta-nerve growth factor	Beta-NGF
Brain-derived neurotrophic factor	BDNF
Caspase 8	CASP-8
C-C motif chemokine 4	CCL4
C-C motif chemokine 19	CCL19
C-C motif chemokine 20	CCL20
C-C motif chemokine 23	CCL23
C-C motif chemokine 25	CCL25
C-C motif chemokine 28	CCL28
CD40L receptor	CD40
CUB domain-containing protein 1	CDCP1
C-X-C motif chemokine 1	CXCL1
C-X-C motif chemokine 5	CXCL5
C-X-C motif chemokine 6	CXCL6
C-X-C motif chemokine 9	CXCL9
C-X-C motif chemokine 10	CXCL10
C-X-C motif chemokine 11	CXCL11
Cystatin D	CST5
Delta and Notch-like epidermal growth factor-related receptor	DNER
Eotaxin-1	CCL11
Eukaryotic translation initiation factor 4E-binding protein 1	4E-BP1
Fibroblast growth factor 5	FGF-5
Fibroblast growth factor 19	FGF-19
Fibroblast growth factor 21	FGF-21
Fibroblast growth factor 23	FGF-23
Fms-related tyrosine kinase 3 ligand	Flt3L

Fractalkine	CXC3CL1
Glial cell line-derived neurotrophic factor	hGDNF
Hepatocyte growth factor	HGF
Intereron gamma	IFN-gamma
Interleukin-1 alpha	IL-1 alpha
Interleukin-2	IL-2
Interleukin-2 receptor subunit beta	IL-2RB
Interleukin-4	IL-4
Interleukin-5	IL-5
Interleukin-6	IL-6
Interleukin-7	IL-7
Interleukin-8	IL-8
Interleukin-10	IL-10
Interleukin-10 receptor subunit alpha	IL-10RA
Interleukin-10 receptor subunit beta	IL-10RB
Interleukin-12 subunit beta	IL-12B
Interleukin-13	IL-13
Interleukin-15	IL-15RA
Interleukin-17A	IL-17A
Interleukin-17C	IL-17C
Interleukin-18	IL18
Interleukin-18 receptor 1	IL-18R1
Interleukin-20	IL-20
Interleukin-20 receptor subunit alpha	IL-20RA
Interleukin-22 receptor subunit alpha-1	IL-22 RA1
Interleukin-24	IL-24
Interleukin-33	Il-33
Latency-associated peptide transforming growth factor beta 1	LAP TGF-beta-1
Leukemia inhibitory factor	LIF
Leukemia inhibitory factor receptor	LIF-R
Macrophage colony-stimulating factor	CSF-1
Macrophage inflammatory protein 1-alpha	MIP-1 alpha
Matrix metalloproteinase-1	MMP-1
Matrix metalloproteinase-10	MMP-10
Monocyte chemotactic protein 1	MCP-1
Monocyte chemotactic protein 2	MCP-2
Monocyte chemotactic protein 3	MCP-3
Monocyte chemotactic protein 4	MCP-4
Natural killer cell receptor 2B4	CD244
Neurotrophin-3	NT-3
Neurturin	NRTN

oncostatin-M	OSM
osteoprotegerin	OPG
Programmed cell death 1 ligand 1	PD-L1
Protein S100-A12	EN-RAGE
Signalling lymphocytic activation molecule	SLAMF1
SIR2-like protein 2	SIRT2
STAM-binding protein	STMPB
Stem cell factor	SCF
Sulfotransferase 1A1	ST1A1
T-cell surface glycoprotein CD5	CD5
T-cell surface glycoprotein CD6 isoform	CD6
Thymic stromal lymphopoietin	TSLP
TNF-beta	TNFB
TNF-related activation-induced cytokine	TRANCE
TNF-related apoptosis-inducing ligand	TRAIL
Transforming growth factor alpha	TGF-alpha
Tumour necrosis factor ligand superfamily member 12	TWEAK
Tumour necrosis factor	TNF
Tumour necrosis factor ligand superfamiliy member 14	TNFSF14
Tumour necrosis factor receptor superfamily member 9	TNFRSF9
Urokinase-type plasminogen activator	uPA
Vascular endothelial growth factor A	VEGF-A

Supplementary Table 3. Comparison of the mean body mass index (BMI) over time. It showed that at week 4 the mean BMI was not significantly different from the mean BMI prior to FMT. At week 12, patients had significantly higher BMI relative to pre-FMT, but did not exceed pre-rCDI baseline.

	Mean BMI Difference (95% CI)	**P Value**
Week 4 - Pre-FMT	0.0 (-0.3, 0.3)	0.84
Week 12 - Pre-FMT	0.5 (0.2, 0.8)	0.003
Week 12 - Week 4	0.4 (0.1, 0.8)	0.006

Response to Reviewers re Submission to *Gut Microbes,* KGMI-20180038, "Effective fecal microbiota transplantation for recurrent *Clostridium difficile* infection in humans is associated with increased signalling in bile acid-farnesoid X receptor-fibroblast growth factor pathway"

Reviewer #2: I would like to thank the authors for revising the manuscript. This is an excellent study with potentially important findings regarding the role of Fgf19 and bile acid signaling in rCDI recovery. I have only two minor suggestions for improvement:

Figs 1 and 2: The labeling on the x-axis is somewhat confusing, and providing the BA or gene name as a title above the chart may make these figures easier to read.

Supplementary Table 2 should be S Table 1, since it is referenced first in the text.

Response: Thank you so much for these comments. We agree with your suggestions and have revised Figure 1 and Figure 2 to make it easier for readers to understand. We have also changed supplementary Table 2 to supplementary Table 1, and changed supplementary Table 1 to supplementary Table 2 both in the manuscript and in the supplementary material.